

# Detection of structural damage via free vibration responses generated by approximating artificial neural networks

C.Y. Kao <sup>a</sup>, Shih-Lin Hung <sup>b,\*</sup>

<sup>a</sup> National Center for Research on Earthquake Engineering, 200 Sec. 3, Hsinhai Road, Taipei, Taiwan, ROC

<sup>b</sup> Department of Civil Engineering, National Chiao Tung University, 1001 Ta Hsueh Road, Hsinchu 300, Taiwan, ROC

Accepted 8 July 2003

## Abstract

This work presented a novel neural network-based approach for detecting structural damage. The proposed approach involves two steps. The first step, system identification, uses neural system identification networks (NSINs) to identify the undamaged and damaged states of a structural system. The second step, structural damage detection, uses the aforementioned trained NSINs to generate free vibration responses with the same initial condition or impulsive force. Comparing the periods and amplitudes of the free vibration responses of the damaged and undamaged states allows the extent of changes to be assessed. Furthermore, numerical and experimental examples demonstrate the feasibility of applying the proposed method for detecting structural damage.

© 2003 Elsevier Ltd. All rights reserved.

**Keywords:** Neural networks; Structural damage detection; Free vibration responses; System identification; Shaking table test; Structural health monitoring

## 1. Introduction

Civil engineering structures are prone to damage and deterioration during their service life. Damage assessment attempts to determine whether structural damage has occurred, as well as the location and extent of any such damage. However, detecting structural damage and identifying damaged elements in a large complex structure are challenging tasks since the in situ measured data of large civil engineering structures such as bridges and buildings are inaccurate (owing to noise corruption) and often incomplete (for economy consideration).

Conventional damage assessment methods [1,2] are inevitably direct process methods, proceeding linearly from causes to effects. These methods involve first constructing a mathematical model for the structure, and

then applying that model to elucidate structural behavior and establish correlations between specific member damage conditions and changes in structural response. Despite their many attractive features, conventional damage assessment methods may encounter difficulties, such as measurement noise and modeling errors, when detecting difficult to model systems. Additionally, commonly adopted damage assessment algorithms are generally complex and inappropriate where measured data are inappropriate.

The artificial neural network (ANN) model is robust and fault tolerant [3–5]. ANN can also effectively deal with qualitative, uncertain, and incomplete information, making it highly promising for detecting structural damage. The feasibility of applying these networks to detect structural damage has received considerable attention. Wu et al. [6] employed spectral acceleration, generated from a numerical model of a simple frame, as an input to a neural network. Based on their results, ANNs can learn about the behavior of undamaged and damaged structures to identify the damaged portions

\* Corresponding author. Tel.: +886-3-5731907; fax: +886-3-5717417.

E-mail address: [slhung@cc.nctu.edu.tw](mailto:slhung@cc.nctu.edu.tw) (S.-L. Hung).

and the extent of the damage from patterns in the frequency response of the structure. When using ANNs trained with samples generated from a finite element model, Elkordy et al. [7] diagnosed damage states obtained experimentally from a series of shaking-table tests involving a five-story steel frame. Despite promising results of their case study, Elkordy et al. indicated the need for further study of the relation between the number of damage patterns required to train the network to perform satisfactorily and the degree of simplification of the model. Meanwhile, Szezyk and Hajela [8] used a modified counter-propagation neural network to develop the inverse mapping between a vector of the stiffness of individual structural elements and the vector of the global static displacements under a testing load. Their case study results showed that the network functions as an associative memory device capable of achieving satisfactory diagnostics even with noisy or incomplete measurements. Pandey and Barai [9] examined the feasibility of applying multi-layer perceptron to detect structural damage to a steel bridge based on the static vertical displacements of nodes.

Extending upon previous investigations by addressing a class of problems where the failure states are unknown, Masri et al. [10,11] and Hung and Kao [12] presented nonparametric structural damage detection methodologies based on system identification approaches for monitoring the health of a structure-unknown system. The approach of Masri et al. [10,11] relies on using vibration measurements from a “healthy” system to train an ANN for identification purposes. Subsequently, comparable vibration measurements from the same structure under different episodes of response are inputted to the trained network to monitor the health of the structure. By utilizing the predictions of the ANN before and after potential structural changes (damage) in the physical system have occurred, quantifiable measures of the degree of fidelity of the predicted response measurements can be used to assess the extent of changes. Hung and Kao [12] demonstrated that partial derivatives of the outputs with respect to the inputs of the approximating ANN (functions of weights and activation function), which identifies the system in a certain undamaged or damaged state, vary little with system error. Comparing the partial derivatives of the neural system identification network that identify a certain damaged state with those that identify the undamaged state allows the detection of changes to the physical system from its undamaged state.

The periods and amplitudes of a structural free vibration responses contain information on structural properties, meaning structural damage can be detected based on changes in the periods and amplitudes of the structural free vibration response. This work develops a neural network-based approach for detecting changes in

the characteristics of structure-unknown systems. The proposed approach involves two steps. The first step, system identification, uses neural system identification networks (NSINs) to identify the undamaged and damaged states of a structural system. The second step, structural damage detection, uses the aforementioned trained NSINs to generate free vibration responses with the same initial condition or impulsive force. Comparing the periods and amplitudes of the free vibration response of the damaged state with those of the undamaged state allows changes to the physical system from its undamaged state to be detected. Moreover, numerical and experimental examples are presented to demonstrate the feasibility of using the proposed method to detect structural damage.

## 2. Artificial neural networks

Among the many different types of ANN, the feed forward, multilayered, supervised neural network with the error backpropagation algorithm, generally known as the backpropagation (BP) network [5], is by far the most commonly applied owing to its simplicity. Before an ANN can be applied, it needs to learn or be trained from an existing training set comprising pairs of input–output elements. The training of a supervised neural network using BP learning algorithm usually involves two stages, the first of which is the data feed forward. The output of each node is defined as

$$\text{net}_j = \sum_{i=1}^n W_{ij} O_i + \theta_j \quad (1)$$

$$O_j = f(\text{net}_j) \quad (2)$$

where  $W_{ij}$  denotes the weight associated with the  $i$ th node in the preceding layer to the  $j$ th node in the current layer;  $O_i$  represents the output of the  $i$ th node in the preceding layer;  $\theta_j$  is the threshold value of node  $j$  in the current layer;  $O_j$  denotes the output of node  $j$  in the current layer; and function  $f$  represents the activation function. Herein, a nonlinear activation function is used and defined as

$$f(x) = \begin{cases} 1 & x > 1 \\ x & -1 \leq x \leq 1 \\ -1 & x < -1 \end{cases} \quad (3)$$

The second stage is error backpropagation and adjustment of the network weights. The training process applies the system error function to monitor the learning performance of the network. This system error function is defined as

$$E = \frac{1}{2P} \sum_{p=1}^P \sum_{n=1}^N (d_{pn} - o_{pn})^2 \tag{4}$$

where  $P$  denotes the number of instances in the training set, while  $d_{pn}$  and  $o_{pn}$  represent the desired and calculated output of the  $n$ th output node for the  $p$ th instance, respectively. The standard BP algorithm employs a gradient descent approach with a constant step length (learning ratio  $\eta$ ) to train the network.

$$W_{ij,k+1} = W_{ij,k} + \Delta W_{ij,k};$$

$$\Delta W_{ij,k} = -\eta \frac{\partial E}{\partial W_{ij,k}} = -\eta \mathbf{g}_k \tag{5,6}$$

The suffix index  $k$  denotes the  $k$ th learning iteration. However, BP supervised neural network learning models always take a long time to learn. Moreover, the convergence of a BP neural network is highly dependent upon the use of a learning rate ( $\eta$ ). Consequently, several different approaches are developed herein to enhance the learning performance of the BP learning algorithm [3].

Hung and Lin [13] developed a more effective adaptive limited memory Broyden–Fletcher–Goldfarb–Shanno (L-BFGS) learning algorithm based on the approach of a L-BFGS quasi-Newton second-order method [14,15] with an inexact line search algorithm. This algorithm achieved a superior convergence rate to the BP learning algorithm by using second-order derivatives of the system error function with respect to the network weights. In a quasi-Newton method, the Hessian matrix, containing the second-order derivatives of the system error function with respect to the network weights  $\frac{\partial^2 E}{\partial w_i \partial w_j}$ , has to be calculated first. Then, the inverse of the Hessian matrix must be obtained to determine the search direction. Quasi-Newton, or variable-metric, methods determine the search direction  $\mathbf{d}_k$  by multiplying the gradient of the function  $E$ ,  $\mathbf{g}_k$ , by the inverse of a matrix that approximates the Hessian matrix of  $E$  at  $\mathbf{W}_k$ :

$$\mathbf{d}_k = -\mathbf{H}_k^{-1} \mathbf{g}_k \tag{7}$$

For the purpose of computational efficiency, a suitable approximation is made and  $\mathbf{H}_k$  is updated during every learning iteration by a correction of the form. Also, the matrix  $\mathbf{H}_k$  must remain symmetric and positive definite, and the quasi-Newton condition. The most common method of update approach is BFGS-update and the approximation  $\mathbf{H}_{k+1}$  to the inverse Hessian matrix of function  $E(\mathbf{W})$  is updated by

$$\mathbf{H}_{k+1} = (\mathbf{I} - \rho_k \mathbf{s}_k \mathbf{y}_k^T) \mathbf{H}_k (\mathbf{I} - \rho_k \mathbf{y}_k \mathbf{s}_k^T) + \rho_k \mathbf{s}_k \mathbf{s}_k^T$$

$$\equiv \mathbf{V}_k^T \mathbf{H}_k \mathbf{V}_k + \rho_k \mathbf{s}_k \mathbf{s}_k^T \tag{8}$$

where

$$\rho_k = 1/\mathbf{y}_k^T \mathbf{s}_k, \quad \mathbf{V}_k = \mathbf{I} - \rho_k \mathbf{y}_k \mathbf{s}_k^T,$$

$$\mathbf{s}_k = \mathbf{W}_{k+1} - \mathbf{W}_k, \quad \mathbf{y}_k = \mathbf{g}_{k+1} - \mathbf{g}_k, \tag{9-13}$$

and  $\mathbf{g}_k = \frac{\partial E}{\partial \mathbf{W}}$

Instead of forming the matrix  $\mathbf{H}_k$  with the BFGS method, the vectors  $\mathbf{s}_k$  and  $\mathbf{y}_k$  are saved. These vectors first define and then implicitly and dynamically update the Hessian approximation using information from the last few iterations, referred to herein as  $m$ . Therefore, the final stage of the adjustment of the weights in a BP-based ANN is modified as follows:

$$\mathbf{W}_{k+1} = \mathbf{W}_k + \alpha_k \mathbf{d}_k \tag{14}$$

The search direction is given by

$$\mathbf{d}_k = -\mathbf{H}_k \mathbf{g}_k + \beta_k \mathbf{d}_{k-1} \tag{15}$$

where

$$\beta_k = \frac{\mathbf{y}_{(k-1)}^T \mathbf{H}_{(k-1)} \mathbf{g}_{(k-1)}}{\mathbf{y}_{(k-1)}^T \mathbf{d}_{(k-1)}} \tag{16}$$

The step length,  $\alpha_k$ , is adapted during the learning process through a mathematical approach: the inexact line search algorithm. This approach is used in the L-BFGS learning algorithm instead of a constant learning ratio [13]. The inexact line search algorithm is based on three sequential approaches: bracketing, sectioning, and interpolation. The bracketing approach brackets the potential step length,  $\alpha$ , between two points, through a series of function evaluations. The sectioning approach then uses the two points of the bracket as the initial points, reducing the step size piecemeal, and locating the minimum between points, such as,  $\alpha_1$  and  $\alpha_2$ , to a specified degree of accuracy. Finally, the quadratic interpolation approach uses the three points,  $\alpha_1$ ,  $\alpha_2$  and  $(\alpha_1 + \alpha_2)/2$ , to fit a parabola to determine the step length,  $\alpha_k$ . The problem of selecting a learning ratio through trial and error in the BP algorithm is thus circumvented in the adaptive L-BFGS learning algorithm.

### 3. Damage detection strategy

This study presents a neural network-based approach for detecting changes in the characteristics of structure-unknown systems. This approach, as shown in Fig. 1, involves two steps. The first step, system identification, uses neural system identification networks (NSINs) to identify the undamaged and damaged states of a structural system. The second step, structural damage detection, uses the aforementioned trained NSINs to generate free vibration responses with the same initial condition or impulsive force. Comparing the periods

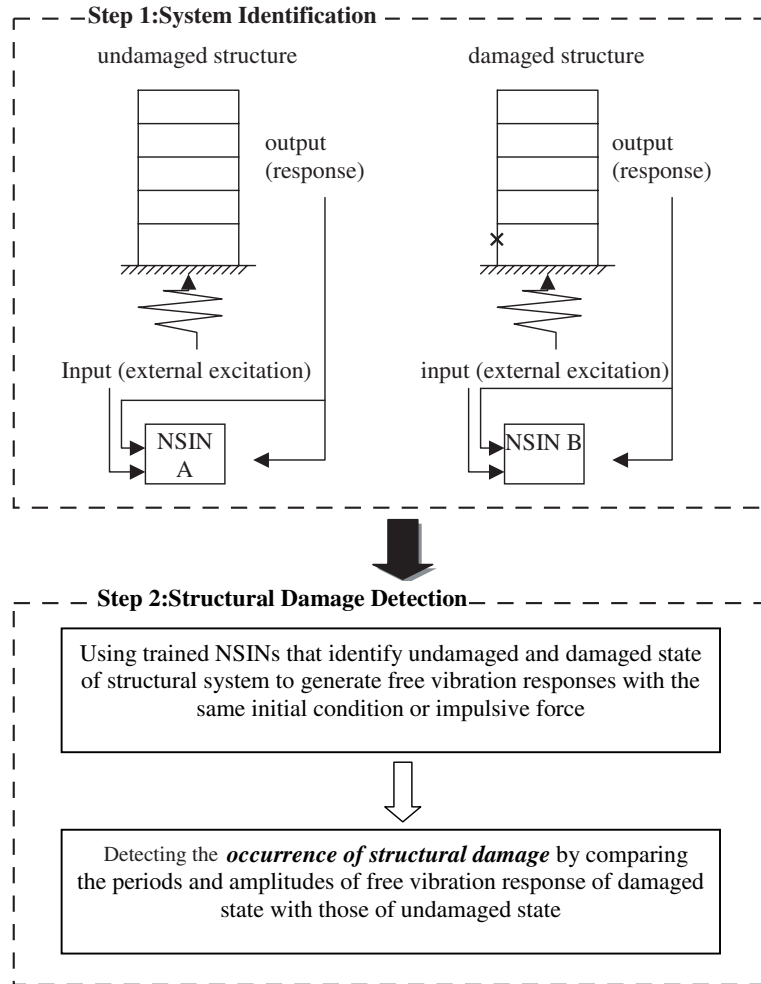


Fig. 1. Schematic diagram of the proposed approach.

and amplitudes of the free vibration response of the damaged and undamaged states can reveal the extent of changes. The following presents the details of the above approaches.

### 3.1. Neural system identification networks

ANN models have been extensively applied to identify dynamic systems. Cybenko [16] and Funahashi [17] rigorously demonstrated that, even with only one hidden layer, neural networks can uniformly approximate any continuous function. Consequently, this theoretical basis for modeling linear or nonlinear systems by neural networks is sound. Making some mild assumptions, a discrete-time multivariable linear or nonlinear time-invariant structural system with  $r$  inputs (external excitations) and  $m$  outputs (including relative displacements, velocities and accelerations) can be represented by the following equation:

$$y(k) = g(y(k-1), \dots, y(k-n_y), p(k), \dots, p(k-n_p)) \tag{17}$$

where

$$p(k) = [p_1(k) \ \dots \ p_r(k)]^T \tag{18}$$

and

$$y(k) = [y_1(k) \ \dots \ y_m(k)]^T \tag{19}$$

$$= [d_1(k) \ v_1(k) \ a_1(k) \ \dots \ d_m(k) \ v_m(k) \ a_m(k)]^T \tag{20}$$

are the system input and output vectors, respectively;  $n_p$  and  $n_y$  denote the maximum lags in the input and output, respectively; index  $k$  represents an integer number;  $k = 0, 1, 2, \dots, N$ ;  $d(k)$ ,  $v(k)$  and  $a(k)$  are, respectively, the relative displacement, velocity and acceleration vectors of the system at time  $t = k\Delta t$ , where  $\Delta t$  is the length of the sampling period; and  $g$  denotes some vector-valued linear or nonlinear function.

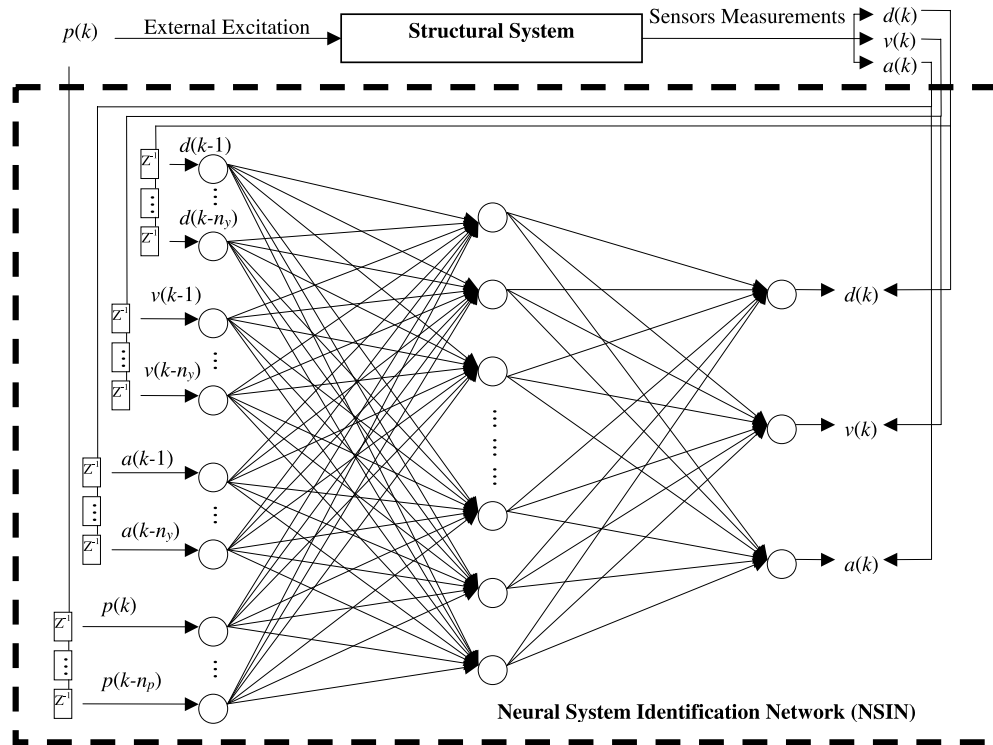


Fig. 2. The architecture of the neural structural identification network.

Function  $g$  in Eq. (17) can be approximated with the ANN, called the neural system identification network (NSIN), as illustrated in Fig. 2. The inputs of the NSIN are relative displacements, velocities, and accelerations in  $(k-1)$  back-to  $(k-n_y)$  time steps, and external excitations in  $k$  back-to  $(k-n_p)$  time steps. These inputs are denoted as  $d_1(k-1), \dots, d_m(k-1), \dots, d_1(k-n_y), \dots, d_m(k-n_y)$  for relative displacements,  $v_1(k-1), \dots, v_m(k-1), \dots, v_1(k-n_y), \dots, v_m(k-n_y)$  for relative velocities,  $a_1(k-1), \dots, a_m(k-1), \dots, a_1(k-n_y), \dots, a_m(k-n_y)$  for relative accelerations, and  $p_1(k), \dots, p_r(k), \dots, p_1(k-n_p), \dots, p_r(k-n_p)$  for external excitations. Meanwhile, the outputs of the NSIN are relative displacements, velocities, and accelerations in the  $k$ th time step and denoted as  $d_1(k), \dots, d_m(k), v_1(k), \dots, v_m(k)$  and  $a_1(k), \dots, a_m(k)$ , respectively. Notably, approximation by the NSIN in a discrete linear system is analogous to identifying the mass, damping and stiffness coefficients in the equation of motion. The NSIN is implemented herein through an adaptive L-BFGS neural network model.

### 3.2. Generating a free vibration response using the trained NSIN

The periods and amplitudes of a structural free vibration response contain information on structural properties, meaning it is feasible to detect structural

damage from changes in the periods and amplitudes of the structural free vibration response. However, generating a structural free vibration is difficult if the structural properties are unknown. Recently, Hung et al. [18] have developed a method for simulating the seismic response of a nonlinear hysteretic structure using the approximating ANN. This approach can be used to generate the free vibration response of a structure-unknown system. The generation on a free vibration response using the trained NSIN which identifies the undamaged or damaged state of the system is as follows:

- (1) Provide an initial input vector (initial condition or impulsive force) to the trained NSIN.
- (2) Feed forward the initial input vector in step (1) through the trained NSIN to compute the output vector.
- (3) Feed back this computed output vector to the input layer of the trained NSIN as the next input vector.
- (4) Feed forward the next input vector in step (3) through the trained NSIN to compute the next output vector.
- (5) Return to step (3) and repeat until the maximal number of iterations is reached.

The free vibration response generated by the NSIN which identifies the undamaged state and is compared to

that generated by the NSIN which identifies the damaged state. If the network has been well trained, and if the system characteristics have not changed, the periods and amplitudes of both free vibration responses will match. On the other hand, if the system has changed, the above statement will no longer stand. The deviations between the periods and amplitudes of the two free vibration responses provide a quantitative measure of the changes in the physical system relative to its “healthy” condition.

## 4. Illustrative examples

### 4.1. Example 1: The numerical example

In this example, a five-story shear building was chosen to demonstrate the feasibility of using the proposed approach to detect the damage of linear MDOF structure systems. The structural properties of the building are assumed to be as follows: floor mass  $m = 8 \times 10^4$  kg, floor stiffness  $k = 4 \times 10^7$  N/m, and floor damping  $c = 1.5 \times 10^6$  Ns/m for all floors. EL-Centro earthquake was used as the external excitation. The sampling period  $\Delta t$  is 0.01 second. In this example, only the relative acceleration time histories of the five floors, computed by state space procedure (SSP), were used as measured responses of the structure.

First, relations between the changes of structural properties (floor stiffness and damping) and those of the periods and amplitudes of the structural free vibration response were discussed. Fig. 3 shows the comparison of the free vibration responses (relative accelerations), with initial ground acceleration 0.01g, of three cases (floor stiffness reduction varies from 0% to 40% every 20%) between 0.5 and 6.5 s. It shows that the more the floor stiffness reduction, the longer the periods of the free vibration response. Fig. 4 shows the comparison of the free vibration responses, with initial ground acceleration 0.01g, of the three cases (floor damping increase varies from 0% to 40% every 20%) between 0.5 and 6.5 s. It shows that the more the floor damping increase, the smaller the amplitudes of the free vibration response.

Second, the undamaged case was used to compare the free vibration response generated by the trained NSIN with the numerical solution (computed by SSP). The training data set of the NSIN is the 2000 records of EL-Centro Earthquake. The NSIN consists of 301, 0, and 5 nodes in input layer, hidden layer, and output layer, respectively, and denoted as NSIN\_L-BFGS(301-0-5). The 301 input data are 250 the structural relative accelerations of the five floors in  $(k - 1)$  back-to  $(k - 50)$  time steps, and 51 external excitations in  $k$  back-to  $(k - 50)$  time steps. The five outputs are the structural relative accelerations of the five floors at time  $k$ . The complete off-line training process took 1000 cycles and the system error converges to  $1.2085 \times 10^{-18}$ . After

training, the NSIN was used to generate free vibration responses of the building system. Fig. 5 is the comparison of the two free vibration responses (between 0.5 and 6.5 s) with initial ground acceleration 0.01g, which shows the excellent correspondence between the numerical solutions and the generated free vibration responses from the trained NSIN for the five floors.

In order to verify the computational efficiency of L-BFGS learning algorithm, NSIN\_BP(301-0-5) with the same topology and training data of NSIN\_L-BFGS(301-0-5) was also used to identify the undamaged case. NSIN\_BP(301-0-5) was implemented using standard BP learning algorithm with a constant learning ratio  $\eta = 0.5$ . The complete off-line training process of NSIN\_BP(301-0-5) took 200,000 cycles and the system error converges to  $3.6109 \times 10^{-9}$ . The CPU (Intel(R) Pentium(R) 4 Mobile CPU 1.60 GHz) times spent by NSIN\_L-BFGS(301-0-5) and NSIN\_BP(301-0-5) are 3496.6 and 22343.0 s, respectively. Results show that L-BFGS learning algorithm converges much faster than standard BP learning algorithm.

### 4.2. Example 2: The experimental example

In this example, the dynamic responses of a five-story steel frame, subjected to various strengths of the Kobe earthquake in shaking table tests, were processed to demonstrate the applicability of the proposed method. This series shaking table tests were undertaken by The National Center for Research in Earthquake Engineering in Taiwan on a 3 m long, 2 m wide, and 6.5 m high steel frame [19] (Fig. 6) to generate a set of earthquake response data for a five-story steel structure. Lead blocks were piled on each floor such that the mass of each floor was approximately 3664 kg. The frames were subjected to the base excitation of the Kobe earthquake, weakened by various levels. The displacements, velocity, and acceleration response histories of each floor were recorded during the shaking table tests. Additionally, some strain gauges were also installed in one of the columns and near the first floor. The sampling rate of the raw data was 1000 Hz.

Notably, it is reported [19] that the frame responded linearly when it subjected to 8%, 10%, 20%, 40%, and 52% of the strength of the Kobe earthquake. Measured strains and visual inspection revealed that 60% of the strength of the Kobe earthquake input caused the steel columns near the first floor to yield.

#### 4.2.1. NSINs training

In the following, only the responses (relative accelerations) and inputs in the long span direction were addressed. The significant responses between 4.5 and 12.5 s were used to train ANNs and thus, to some extent, reduce the noise effect. Five NSINs were used to identify the following five states.

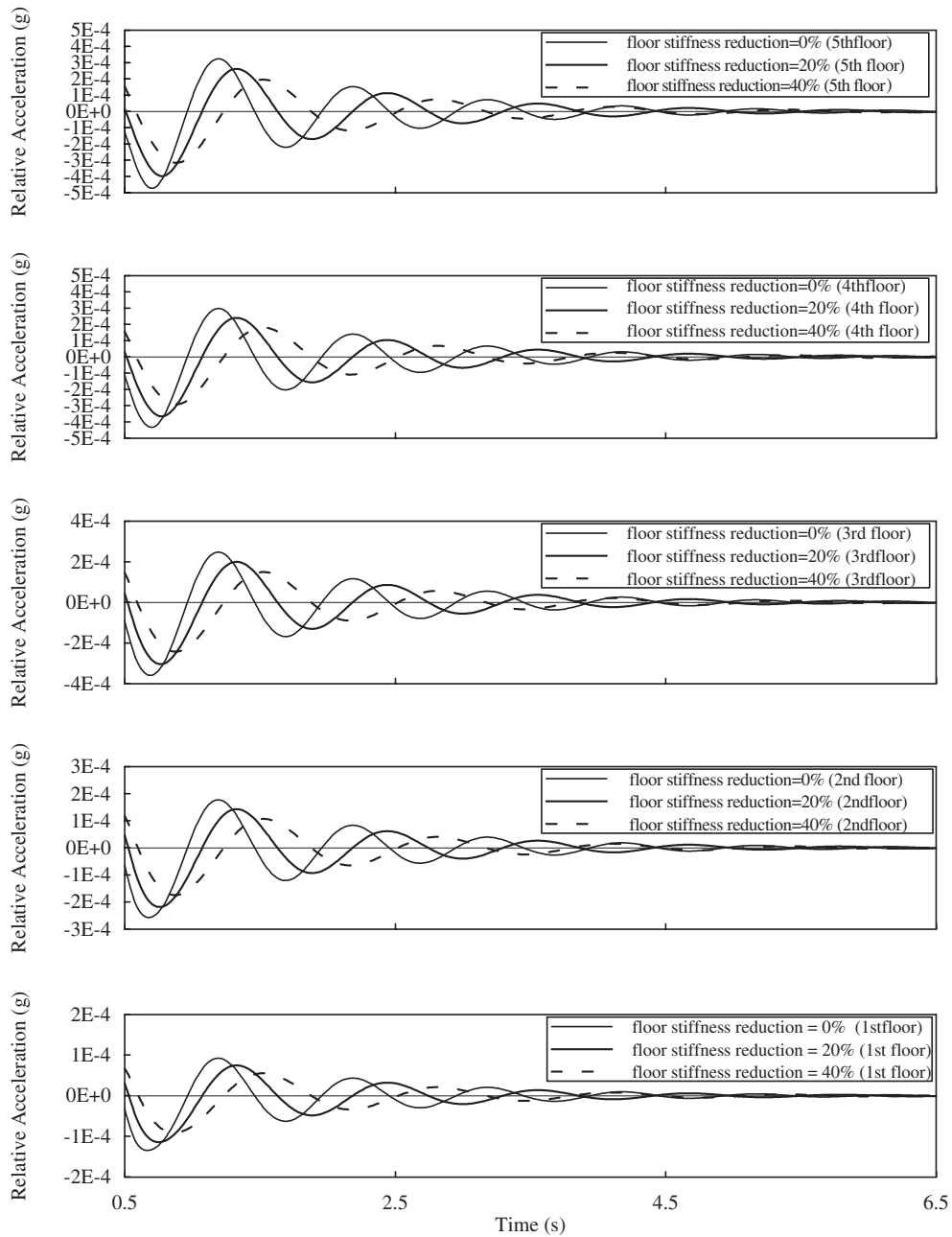


Fig. 3. Comparison of the free vibration responses, with initial ground acceleration 0.01g, of three cases (floor stiffness reduction varies from 0% to 40% every 20%).

- State 1: The frame was subjected to 10% Kobe earthquake.
- State 2: The frame was subjected to 20% Kobe earthquake.
- State 3: The frame was subjected to 40% Kobe earthquake.
- State 4: The frame was subjected to 52% Kobe earthquake.
- State 5: The frame was subjected to 60% Kobe earthquake.

Networks with the same topology of the previous example were employed in this example. That is, the topology of each NSIN is NSIN\_L-BFGS(301-0-5). The 301 inputs and the five outputs are the same as that in the previous example. The complete off-line training

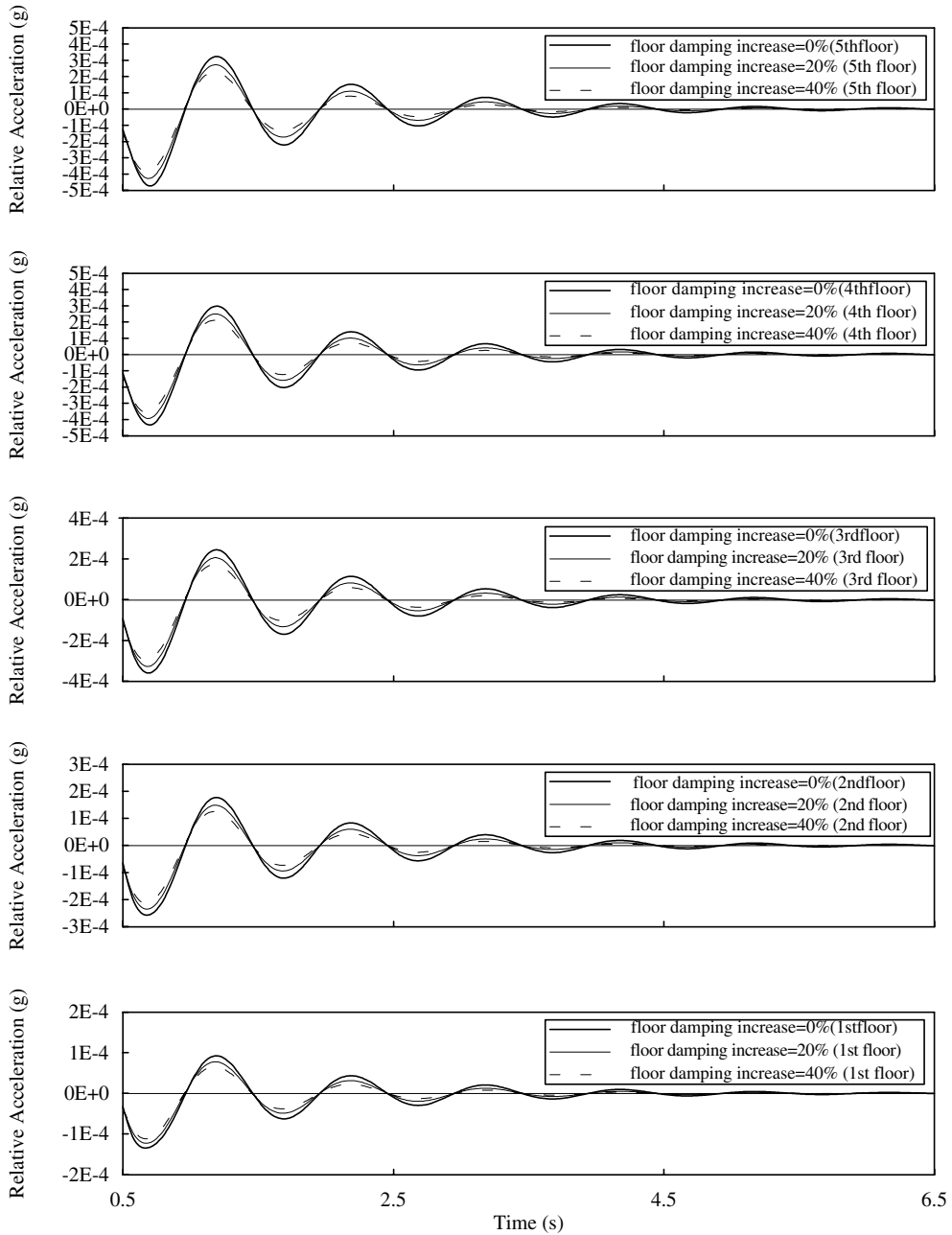


Fig. 4. Comparison of the free vibration responses, with initial ground acceleration 0.01g, of the three cases (floor damping increase varies from 0% to 40% every 20%).

process took 3000 cycles and the system errors of the five NSINs were listed in Table 1.

4.2.2. Detection of structural damage

After training, the five NSINs were used to generate free vibration responses to investigate the changes of the structural properties with excitation magnitude. First,

the comparison of the free vibration responses of state 1, state 2, and state 3, with initial ground acceleration 0.01g, is shown in Fig. 7. It reveals that the periods of the three free vibration responses were almost identical, but the amplitude becomes smaller and smaller with the increasing of excitation magnitude. According to results of Example 1, it shows that the stiffness values of the



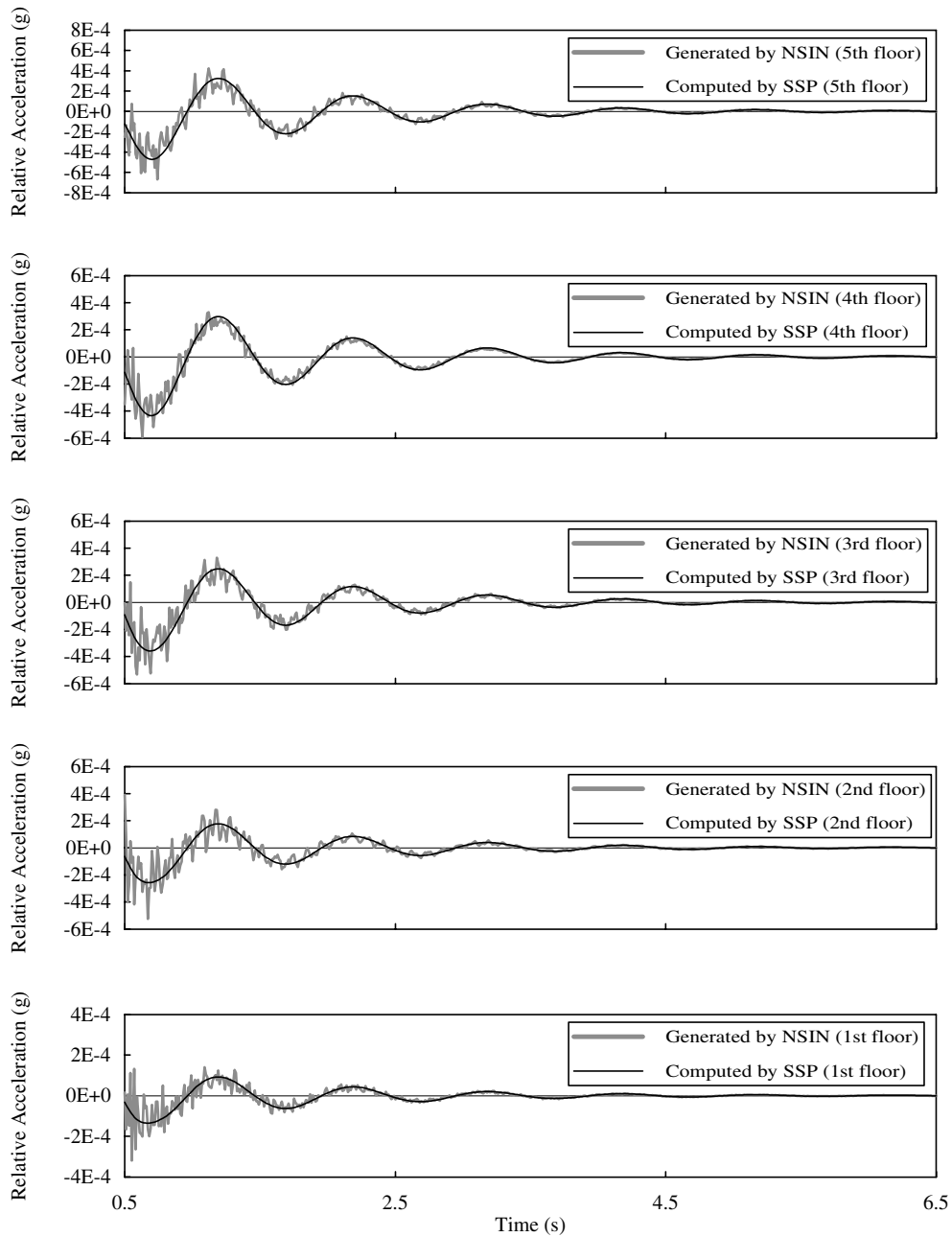


Fig. 5. Comparison of the numerical solutions and generated free vibration responses, with initial ground acceleration 0.01g, from the trained NSIN.

three states were almost the same, and the damping values increase with the increasing of excitation magnitude. Second, the comparison of the free vibration responses of state 3 and state 4, with initial ground acceleration 0.01g, is shown in Fig. 8. It displays that the periods of the free vibration of state 4 were slightly

longer than that of state 3, and the amplitudes of the two free vibration responses were almost the same. According to results of example 1, it exposes that the stiffness values of state 4 were a little smaller than those of state 3, but the damping values of the two states were almost the same. Finally, the comparison of the free vibration

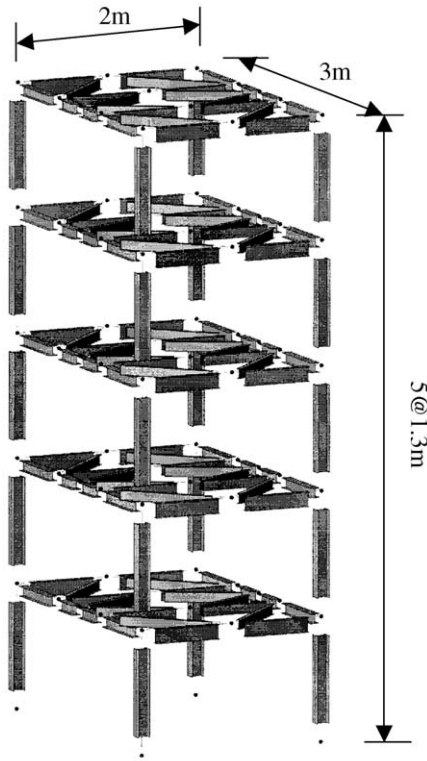


Fig. 6. Simple sketch of a five-story steel frame.

Table 1  
System errors of the five states

State	System error
1	$1.72 \times 10^{-7}$
2	$6.08 \times 10^{-7}$
3	$5.68 \times 10^{-5}$
4	$6.22 \times 10^{-5}$
5	$1.72 \times 10^{-4}$

responses of state 4 and state 5, with initial ground acceleration  $0.01g$ , is shown in Fig. 9. It reveals that the periods of the free vibration of state 5 were longer than those of state 4, and the amplitudes of the free vibration of state 5 were larger than those of state 4. Based on results of example 1, the stiffness and damping values of state 5 were smaller than those of state 4. In addition, it has to be pointed out that the free vibration response of the fifth floor of state 5 obviously deviates the central line (relative acceleration = 0), which may be a message that some elements of the frame were yield under such strong excitation magnitude. The result completely corresponds with the evidence investigated in the lab.

## 5. Conclusions

This study presented a novel neural network-based approach for detecting structural damage. Noteworthy, the proposed approach is practically feasible for structural damage detection. The practical feasibility of the proposed approach is supported by the following two reasons. First, ANNs are a promising tool for damage detection of real-world structures. Second, the results of numerical and experimental examples prove the practical feasibility of the proposed approach for structural damage detection. The following important conclusions can be drawn from the results presented in this research.

1. Changes on structural properties (stiffness and damping) cause changes on periods and amplitudes of the free vibration of the structure system. Therefore, periods and amplitudes of the free vibration are useful indices to reflect changes of structural properties.
2. The proposed approach makes it easy to accurately generate a free vibration response of a structure-unknown system using neural networks.
3. The proposed approach has the ability to detect changes of structural properties. Especially, this approach can reveal clear message when some structure elements were yield, which cannot be achieved by other analytical methods.

Some limitations expected to be complemented in future studies were summarized as follows:

1. A drawback of proposed approach is the accumulation of simulation error. Since the accumulated simulation error was not obvious in results of illustrative examples, this problem was not discussed in this paper. In fact, Hung et al. had addressed a sensitivity analysis method to decrease the accumulated simulation error (in Appendix A). Nevertheless, this interesting topic could be further researched.
2. Future investigations should apply the proposed approach to measurements in the field to examine its capacity to deal with incomplete measurements and noise corruption. Furthermore, the ability of the proposed approach to detect the location of damage should be further researched.

## Acknowledgements

The authors would like to thank the National Science Council of the Republic of China for financially supporting this research under contract no. NSC 89-2211-E009-072. The appreciation is also extended to the National Center for Research on Earthquake Engineering for providing shaking table testing data.

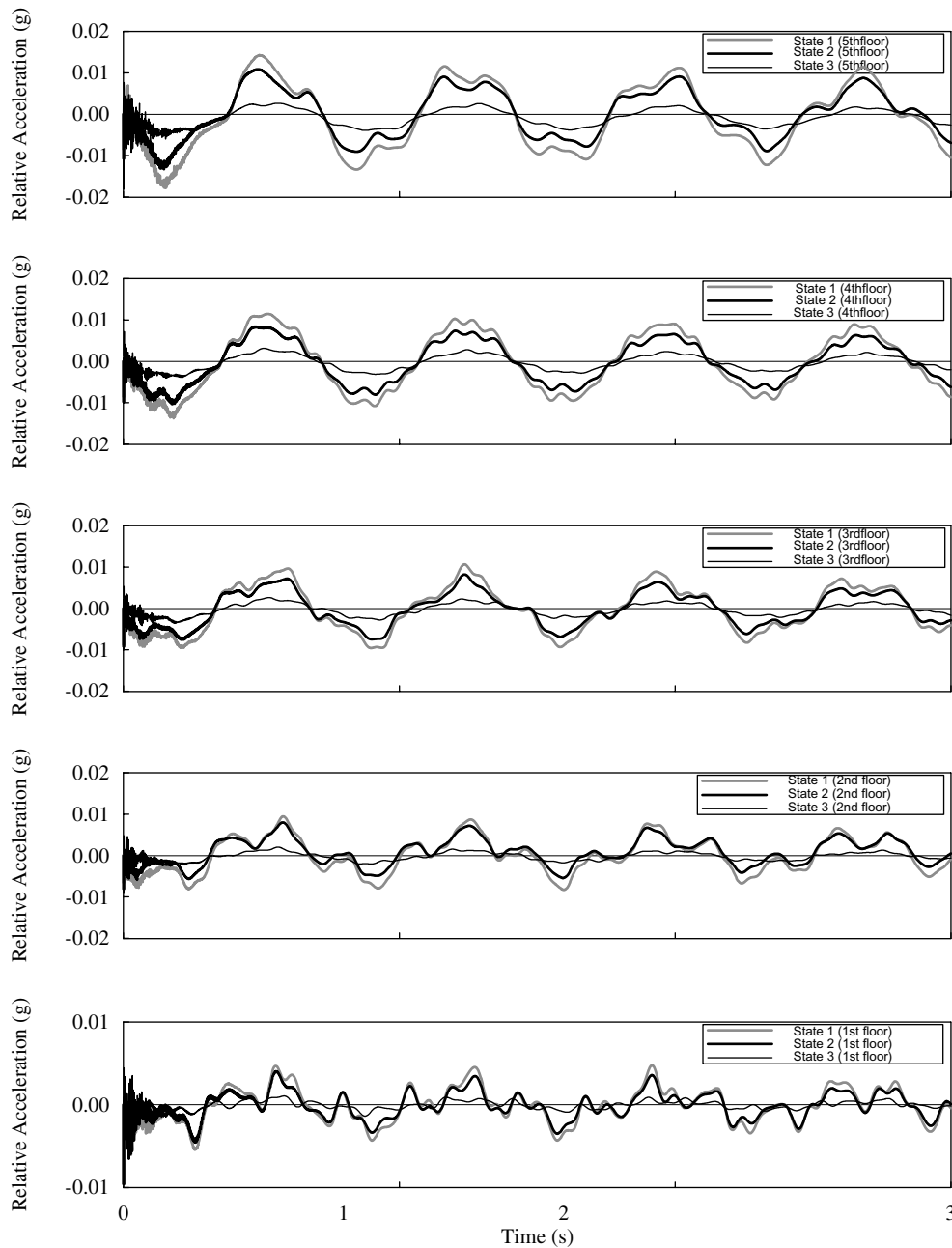


Fig. 7. Comparison of the free vibration responses of state 1, state 2 and state 3, with initial ground acceleration 0.01g.

## Appendix A

The steps of the method developed by Hung et al. [18] for simulating the seismic response of a nonlinear hysteretic structure using the approximating ANN are the same as those described in section “Generating a free vibration response using the trained NSIN”. The only difference is that the external excitation  $p$  is zero (except

in initial input vector) when generating a free vibration using the trained NSIN, while  $p$  is the measured data when simulating the seismic response of a structure using NSIN.

A drawback of this approach is the accumulation of simulation error. Hung et al. had addressed a sensitivity analysis method, as described in the following section, to decrease the accumulated simulation error.

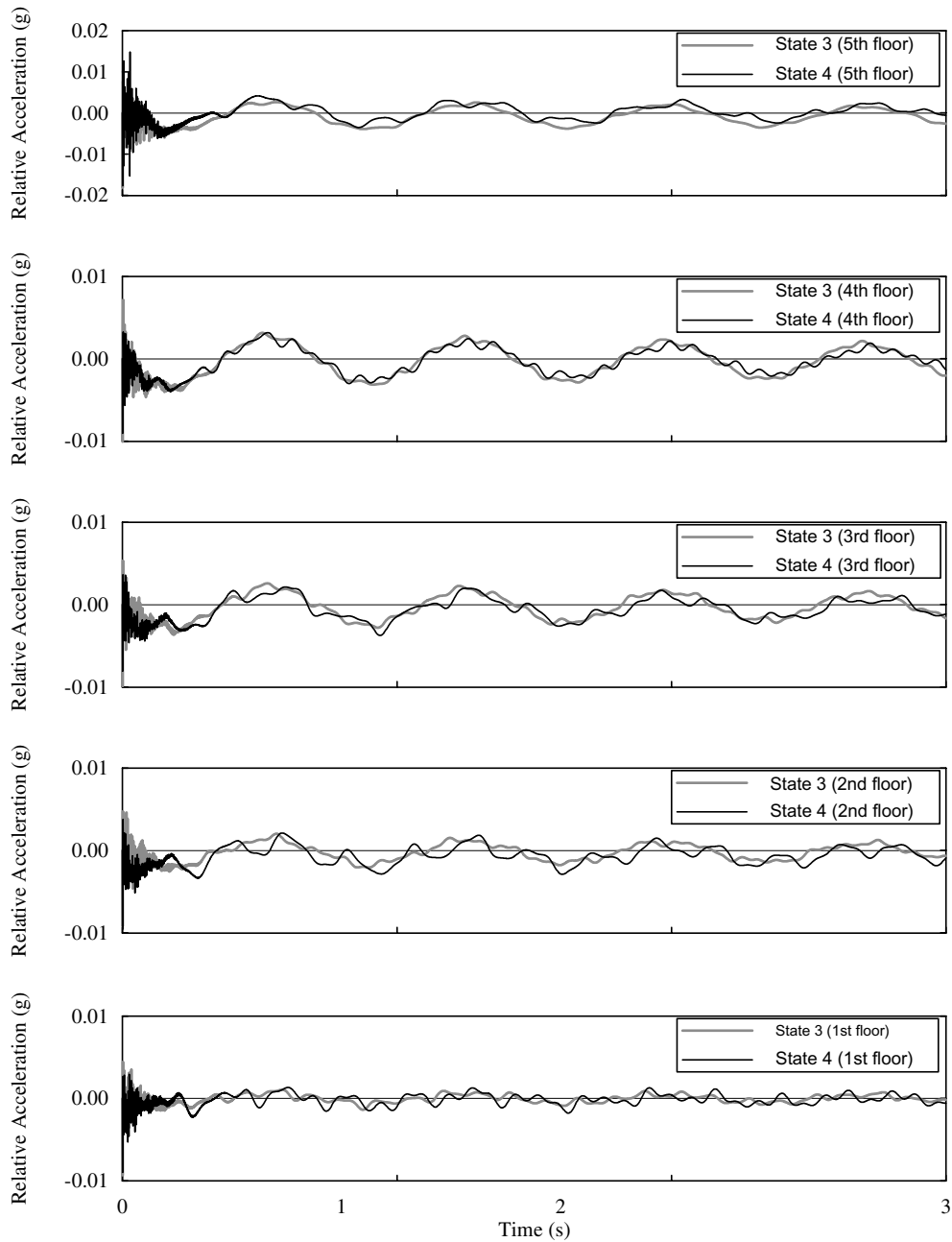


Fig. 8. Comparison of the free vibration responses of state 3 and state 4, with initial ground acceleration 0.01g.

#### A.1. Sensitivity analysis

After an ANN is successfully trained, the relative strength of effect for input element on output data can be derived based on the weights stored in the network. This work adopted a sensitivity index,  $S_{ik}$ , to express the degree of sensitivity for each input

parameter  $x_i$  on one of data in output  $o_k$ . The process of sensitivity analysis was summarized as follows:

1. After an ANN is successfully trained, the computed output for any node then can be yielded through the network and expressed as

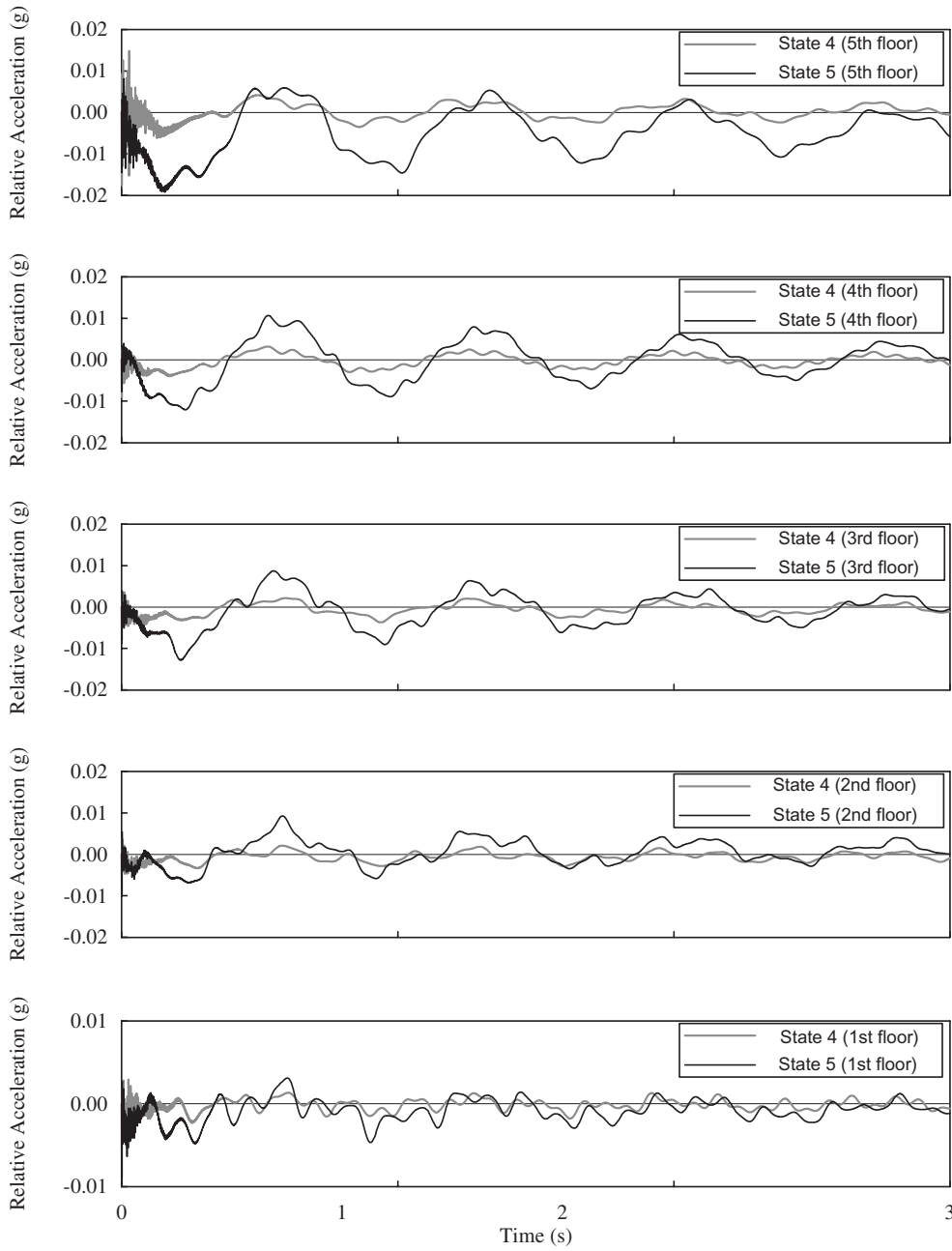


Fig. 9. Comparison of the free vibration responses of state 4 and state 5, with initial ground acceleration 0.01g.

$$o_k = f(\text{net}_k), \quad \text{net}_k = \sum_{j_n} o_{j_n} W_{j_n,k} + \theta_k \quad (\text{A.1})$$

$$o_{j_n} = f(\text{net}_{j_n}), \quad \text{net}_{j_n} = \sum_{j_{n-1}} o_{j_{n-1}} W_{j_{n-1},j_n} + \theta_{j_n} \quad (\text{A.2})$$

$$o_{j_1} = f(\text{net}_{j_1}), \quad \text{net}_{j_1} = \sum_i x_i W_{i,j_1} + \theta_{j_1} \quad (\text{A.3})$$

where  $x_i$  is  $i$ th input parameter; and  $o_k$ ,  $o_{j_n}$ , and  $o_{j_1}$  denote the computed output for output node  $k$ , node  $j_n$  of  $n$ th hidden layer, and node  $j_1$  of first hidden layer, respectively.

2. The variance of output with the change of each input parameter can be derived. The variance is represented by the following equation:

$$\frac{\partial O_k}{\partial x_i} = \sum_{j_n} \sum_{j_{n-1}} \cdots \sum_{j_1} W_{j_n,k} f'(\text{net}_k) W_{j_{n-1},j_n} f'(\text{net}_{j_n}) \cdots W_{i,j_1} f'(\text{net}_{j_1}) \quad (\text{A.4})$$

where  $j_n, j_{n-1}, \dots$ , and  $j_1$  denote hidden nodes in the  $n$ th,  $(n-1)$ th,  $\dots$ , and first hidden layer, respectively;  $W_{j_n,k}$  denotes weight between the  $k$ th output node and hidden node  $j_n$ ;  $W_{j_{n-1},j_n}$  denotes weight between the hidden nodes  $j_{n-1}$  and  $j_n$ ;  $W_{i,j_1}$  denotes weight between the  $i$ th input node and the hidden node  $j_1$ ;  $\text{net}_k, \text{net}_{j_n}$  and  $\text{net}_{j_1}$  denote weighted sums of  $k$ th output node, the hidden node  $j_n$  and  $j_1$  respectively; and  $f'$  denotes differential function of the activation function  $f$ .

3. Sensitivity index,  $S_{ik}$ , is expressed as the average of the total variance of training instances.

$$S_{ik} = \frac{1}{M} \sum_m \left( \frac{\partial O_k}{\partial x_i} \right)_m \quad (\text{A.5})$$

where  $m$  denotes  $m$ th training instances, and  $M$  is the total number of training instances.

4. After computing  $S_{ik}$ , the importance index,  $I_i$ , to express the importance of input  $i$  to outputs can be computed.  $I_i$  is defined as follows:

$$I_i = \sum_k S_{ik} \quad (\text{A.6})$$

Obviously, a large value of  $I_i$  indicates that input  $i$  has more effect on the output data. On the other hand, a small value indicates that input  $i$  has small effect on the output data.

5. After computing  $I_i$ , the trivial input  $i$  of the NSIN is deleted (delete a trivial input at a time) to reduce the number of inputs and enhance the learning speed and accuracy of the NSIN. The trivial input  $i$  is defined as follows:

$$\begin{cases} I_i < I_j & \text{for } j = 1 \sim N \text{ and } j \neq i \\ S_{ik} < S_{jk} & \text{for } j = 1 \sim N \text{ and } j \neq i, \quad k = 1 \sim K \end{cases} \quad (\text{A.7})$$

where  $N$  and  $K$  are the number of inputs and outputs of the NSIN, respectively.

6. After deleting the trivial input of the NSIN, the NSIN is retrained. Sensitivity and importance indices are computed after no trivial input exists. Finally, the seismic response of the structure is simulated using the NSIN with no trivial input.

## References

- [1] Rubin S. Ambient vibration survey of offshore platform. *J Eng Mech*, ASCE 1980;106:425–41.
- [2] Shahrivar F, Bouwkamp JG. Signal separation method for tower mode shape measurement. *J Struct Eng*, ASCE 1989;115:707–23.
- [3] Adeli H, Hung SL. Machine learning—Neural networks, genetic algorithms, and fuzzy systems. New York: Wiley; 1995.
- [4] Suykens J, Vandewalle J, De Moor J. Artificial neural networks for modeling and control of non-linear systems. Boston: Kluwer Academic Publishers; 1996.
- [5] Rumelhart DE, Hinton GE, Williams RJ. Learning international representation by error propagation. In: Rumelhart DE, McClelland JL, the PDP Research Group, editors. Parallel distributed processing. Cambridge, MA: The MIT Press; 1986. p. 318–62.
- [6] Wu X, Ghaboussi J, Garrett Jr JH. Use of neural networks in detection of structural damage. *Comput Struct* 1992; 42(4):649–59.
- [7] Elkordy MF, Chang KC, Lee GC. Neural networks trained by analytically simulated damage states. *J Comput Civil Eng*, ASCE 1993;7(2):130–45.
- [8] Szewczyk P, Hajela P. Damage detection in structures based on feature-sensitivity neural networks. *J Comput Civil Eng*, ASCE 1994;8(2):163–79.
- [9] Pandey PC, Barai SV. Multilayer perception in damage detection of bridge structures. *Comput Struct* 1995;54(4): 597–608.
- [10] Masri SF, Nakamura M, Chassiakos AG, Caughey TK. Neural network approach to detection of changes in structural parameters. *J Eng Mech*, ASCE 1996;122(5): 350–60.
- [11] Masri SF, Smyth AW, Chassiakos AG, Caughey TK, Hunter NF. Application of neural networks for detection of changes in nonlinear systems. *J Eng Mech*, ASCE 2000; 126(7):666–76.
- [12] Hung SL, Kao CY. Structural damage detection using the optimal weights of the approximating artificial neural networks. *Earthquake Eng Struct Dyn* 2002;31:217–34.
- [13] Hung SL, Lin YL. Application of an L-BFGS neural network learning algorithm in engineering analysis and design. In: Proc Second Nat Conf on Struct Engrg. Nantou, Taiwan, ROC; Chinese Society of Structural Engineering; 1994. p. 221–30 [in Chinese].
- [14] Nocedal J. Updating quasi-Newton matrix with limited storage. *Math Comput* 1980;35:20–33.
- [15] Coleman TF, Li Y. Large-scale numerical optimization. Philadelphia: Society for Industrial and Applied Mathematics; 1990.
- [16] Cybenko G. Approximations by superpositions of a sigmoidal function. *Math Control, Signals Systems* 1989; 2:303–14.
- [17] Funahashi K. On the approximate realization of continuous mappings by neural networks. *Neural Networks* 1989;2:183–92.